

Competing superfluid and density-wave ground-states of fermionic mixtures with mass imbalance in optical lattices

Tung-Lam Dao,¹ Antoine Georges,¹ and Massimo Capone²

¹*Centre de Physique Théorique, École Polytechnique, CNRS, 91128 Palaiseau Cedex, France*

²*SMC, CNR-INFN and Dipartimento di Fisica, “Sapienza” Università di Roma, Piazzale Aldo Moro 2, I-00185 Roma, Italy and ISC-CNR, Via dei Taurini 19, I-00185 Roma, Italy*

(Received 2 July 2007; revised manuscript received 27 August 2007; published 24 September 2007)

We study the effect of mass imbalance on the phase diagram of a two-component fermionic mixture with attractive interactions in optical lattices. Using static and dynamical mean-field theories, we show that the pure superfluid phase is stable for all couplings when the mass imbalance is smaller than a limiting value. For larger imbalance, phase separation between a superfluid and a charge-density wave takes place when the coupling exceeds a critical strength. The harmonic trap induces a spatial segregation of the two phases, with a rapid variation of the density at the boundary.

DOI: [10.1103/PhysRevB.76.104517](https://doi.org/10.1103/PhysRevB.76.104517)

PACS number(s): 67.20.+k, 05.30.Fk, 03.75.Lm, 71.10.Fd

I. INTRODUCTION

The remarkable advances in handling ultracold atomic gases have given birth to the new field of “condensed matter physics with light and atoms.” Cold atoms in optical lattices, with tunable and controllable parameters, have been studied in many different contexts (for reviews, see Ref. 1). Mixtures of two-component atoms with different masses (e.g., ⁶Li and ⁴⁰K) introduce an additional parameter, namely, the difference between the hopping amplitudes associated with each species in the optical lattice. This may affect the stability of the possible quantum phases or even induce new ones. Recently, a phase diagram has been worked out in the one-dimensional (1D) case² and in continuum models.³

In this paper, we consider such fermionic mixtures in three dimensions, with an attractive on-site coupling. Using analytical and numerical techniques, we establish a ground-state phase diagram as a function of coupling strength and mass imbalance, in all regimes of couplings. We also consider the experimentally relevant effect of the trap potential, which is shown to induce a spatial segregation between superfluid and density-wave phases.

Under conditions discussed, e.g., in Refs. 1, 4, and 5, fermionic mixtures are described by a Hubbard model,

$$H = - \sum_{\langle i,j \rangle, \sigma} t_{\sigma} (c_{i\sigma}^{\dagger} c_{j\sigma} + \text{H.c.}) - |U| \sum_i n_{i\uparrow} n_{i\downarrow}. \quad (1)$$

The (pseudo)spin index σ refers to the two different species. Feshbach resonances between ⁶Li and ⁴⁰K are currently under investigation,⁶ and it would allow for an attractive interaction with a tunable strength, as assumed in Eq. (1). For an example of heteroatomic resonances in the boson-fermion case, see e.g., Ref. 7. In the following, we consider a bipartite optical lattice made of two interpenetrating (A, B) sublattices arranged such that the neighbors of A sites are all of B type and vice versa (this happens, for instance, in the cubic lattice). For simplicity, we consider an equal number of atoms for each species, leaving for future work the study of imbalanced populations.

The paper is organized as follows: in Sec. II, we anticipate the phase diagram obtained by means of dynamical

mean field theory (DMFT), and we introduce the DMFT method itself; in Sec. III, we discuss the results of weak- and strong-coupling static mean-field methods; in Sec. IV, we consider the effect of the trapping potential within local density approximation; while Sec. V is dedicated to concluding remarks.

II. GENERIC PHASE DIAGRAM AND DYNAMICAL MEAN-FIELD THEORY

In order to study the zero temperature ground-state phase diagram of model (1), we use DMFT,⁸ together with analytical mean-field theory calculations for both weak and strong couplings. Let us anticipate the DMFT phase diagram of the uniform system, displayed in Fig. 1. When the fermions have the same mass, the ground state is a superfluid (SF) for all $|U|$. A competing ordering exists, namely, a charge-density wave (CDW), considered here in the simplest (commensurate) case in which the charge is modulated with an alternating pattern on A and B sublattices. At half-filling, i.e., when the number of fermions is equal to the number of lattice sites ($\langle n_{\uparrow} + n_{\downarrow} \rangle = 1$), it is well known that the SF and CDW states are degenerate. This no longer applies in the “doped” system, in which the number of fermionic atoms no longer coincides with the number of sites in the optical lattice; for equal masses, the SF phase is stabilized by doping for all $|U|$, but a large mass imbalance favors the CDW phase over a SF state in which the Cooper pairs must be formed by fermions with different mobilities.² Hence, the SF/CDW competition becomes more interesting in the presence of mass imbalance. As displayed in Fig. 1, we find that the uniform system has a SF ground state for all values of $|U|$ as long as the mass imbalance $z \equiv (t_{\uparrow} - t_{\downarrow}) / (t_{\uparrow} + t_{\downarrow})$ is smaller than a limiting value z_c (which depends on the average density). For $z > z_c$, a (first-order) phase boundary is crossed as $|U|$ is increased, beyond which the uniform system undergoes a phase separation (PS) between a SF and a CDW phase. As discussed later in this paper, this implies that, in the presence of a harmonic trap, the CDW and SF phases may both exist in different regions of the trap.

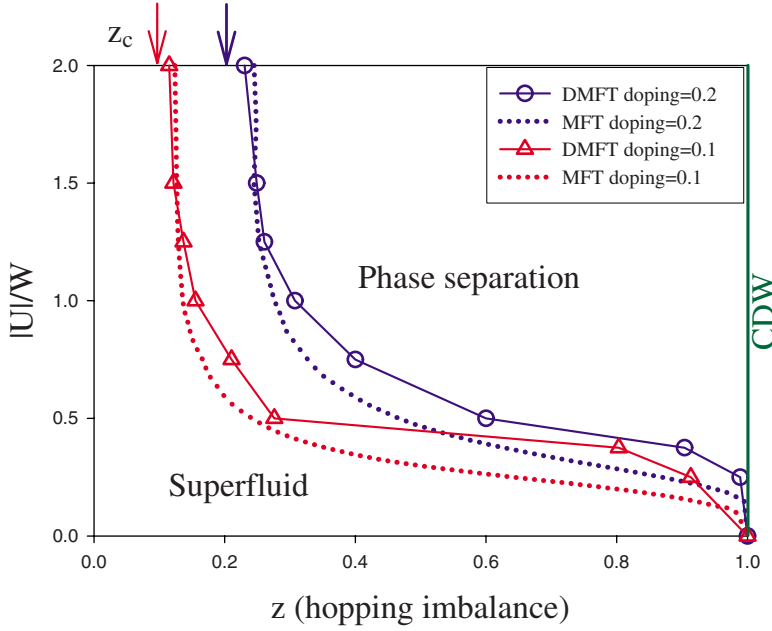


FIG. 1. (Color online) Phase diagram of the uniform system in the $(z, |U|)$ plane obtained from DMFT. Below the curves (displayed here for two “doping” levels $\delta \equiv n-1=0.1, 0.2$), the SF is stable. Above the curves, the system is phase separated into a half-filled CDW and a SF. The arrows indicate the analytical strong-coupling values. The dotted lines are the weak-coupling mean-field approximation (see text). $|U|$ is normalized to the bandwidth W of $(\varepsilon_{\mathbf{k}\uparrow} + \varepsilon_{\mathbf{k}\downarrow})/2$.

DMFT is one of the most popular modern theoretical approaches designed to treat correlated fermions on a lattice. The idea of the method is to extend to the quantum domain the mean-field strategy by replacing the static mean-field averages with frequency-dependent (dynamical) objects. Just like classical mean-field theory, the method freezes the spatial correlations, but the DMFT allows for an unbiased treatment of the dynamics. A practical implementation of DMFT requires the self-consistent solution of a quantum impurity model, i.e., a model of a single interacting site coupled to a bath that allows for quantum fluctuations on the correlated site. In the mean-field spirit, the site is representative of any site of the original lattice. This correspondence is implemented via a self-consistency condition which contains information about the original lattice through the noninteracting density of states. The self-consistency condition relates the frequency-dependent “Weiss field” which describes the dynamics of the bath (analogous to the static Weiss field in mean-field theory of magnetism) $\hat{G}(i\omega)$ entering the effective “impurity model” to the Green’s function.

The general form of the self-consistency equation (we write it for simplicity for the normal metallic phase, but the generalization to the broken-symmetry phases is straightforward) is

$$G(i\omega) = \int d\varepsilon \frac{D(\varepsilon)}{i\omega + \mu - \varepsilon - \Sigma(i\omega)}, \quad (2)$$

where $\Sigma(i\omega) = \mathcal{G}^{-1}(i\omega) - G^{-1}(i\omega)$ is the local self-energy and $D(\varepsilon)$ is the noninteracting density of states. For the case of a semicircular density of states $D(\varepsilon) = 2/\sqrt{(\pi D)\sqrt{4t^2 - \varepsilon^2}}$ with bandwidth $W=4t$, this equation is greatly simplified, and it becomes

$$\mathcal{G}(i\omega) = i\omega + \mu - t^2 G(i\omega). \quad (3)$$

In this work, we use this density of states, which has been shown to satisfactorily reproduce results in $d=3$ in the con-

text of solid state physics. For more details on DMFT, we refer to Ref. 8.

A crucial property of DMFT is that it does not require any assumption on the values of the coupling terms appearing in the Hamiltonian, and it indeed becomes exact both in the small interaction limit and in the strong interaction one. This has been explicitly shown in DMFT studies of the attractive Hubbard model with equal masses, where the crossover from Bardeen-Cooper-Schrieffer superconductivity to Bose-Einstein condensation of preformed pairs has been studied both in the normal⁹ and the superconducting,¹⁰ and both the limiting regimes are basically exactly reproduced.

To describe the superconducting phase, it is convenient to work with Nambu’s spinors $\psi^\dagger = (c_\uparrow^\dagger, c_\downarrow)$. The key quantity in DMFT is the local (on-site) Green’s function, $\hat{G}(\tau) = \langle T_\tau \psi_i(\tau) \psi_i^\dagger(0) \rangle$, and its Fourier transform for imaginary frequencies is

$$\hat{G}(i\omega) = \begin{bmatrix} G_\uparrow(i\omega) & F(i\omega) \\ F^*(i\omega) & -G_\downarrow(-i\omega) \end{bmatrix}, \quad (4)$$

where $G(\tau) = -\langle T c(\tau) c^\dagger(0) \rangle$ is the normal Green’s function on a given site, and $F(\tau) = -\langle T c_\uparrow(\tau) c_\downarrow(0) \rangle$ is the anomalous Green’s function associated with superfluid ordering. The superfluid order parameter is indeed given by $\Delta_{SF} = \langle c_{i\uparrow} c_{i\downarrow} \rangle = F(\tau=0) = \Sigma_\omega F(i\omega)$.

In this work, we also consider the possibility of a CDW state which establishes on our bipartite lattice. In this case, the local Green’s function takes different values (\hat{G}_A and \hat{G}_B) on the two alternating sublattices. The CDW order parameter is the difference of densities on the two sublattices: $\Delta_{CDW} = \langle n_A - n_B \rangle$.

We can generalize the self-consistency of Eq. (3) to the case where both SF and CDW are possible. The result is $\hat{G}_{A(B)}^{-1}(i\omega) = i\omega \hat{1} + \hat{\mu} - \hat{T} \hat{G}_{B(A)}(i\omega) \hat{T}$, in which $\hat{T} = \text{diag}[t_\uparrow, -t_\downarrow]$

and $\hat{\mu} = \text{diag}[\mu_\uparrow, -\mu_\downarrow]$ are diagonal matrices, whose elements are the half-bandwidths and the chemical potentials of the two species.

Since we are able to study all the different broken-symmetry phases, the $T=0$ phase diagram is easily determined by comparing the energies of the different solutions. The energy is evaluated as $\langle H \rangle = \langle K \rangle - |U| \sum_i \langle n_{i\uparrow} n_{i\downarrow} \rangle$. The expectation value of the interaction term is easily computed through the calculation of the expectation value of $\sum_i n_{i\uparrow} n_{i\downarrow}$, while the kinetic energies $\langle K \rangle$ in the SF and CDW phases read $\langle K \rangle_{SF} = \beta^{-1} \sum_{\omega, \sigma} t_\sigma^2 [G_\sigma^2(\sigma i \omega) - F^2(i\omega)]$ and $\langle K \rangle_{CDW} = \beta^{-1} \sum_{\omega, \sigma} t_\sigma^2 G_{A\sigma}(i\omega) G_{B\sigma}(i\omega)$, respectively.

We performed DMFT calculations¹⁴ exploiting the non-perturbative nature of DMFT to span the whole range of coupling $|U|$ and imbalance z . We focused on the vicinity of half-filling and found the phase diagram of the uniform system (Fig. 1) to be qualitatively independent on the ‘‘doping level,’’ i.e., the relative difference between the number of atoms and optical lattice sites, $\delta = \langle n_\uparrow + n_\downarrow - 1 \rangle$. For small enough values $z < z_c(\delta)$ of the mass imbalance, a pure SF solution is stable for all $|U|$. In contrast, for $z > z_c$, the pure SF phase is stable only for small interactions (below the line drawn in Fig. 1). Above this line (which depends on δ), the pure SF solution becomes unstable toward phase separation between a SF and a CDW phase. (Note that we did not find a homogeneous CDW solution out of half-filling, except at $z=1$). This means that it is more convenient to separate the system into a fraction $1-x$ with CDW order and $\delta=0$ and a fraction x with SF order accommodating the rest of the particles. This conclusion is reached by minimizing over x the expression $E_{PS}(x) = (1-x)E_{CDW} + xE_{SF}$. We note that the SF phase is more stable than in the 1D case² (in which nesting favors a CDW with $\mathbf{Q}=2k_F$). We underline that this diagram has been obtained by comparing the energies of the different possible states (normal, SF, and CDW), and that a normal ground state is never stable, either as a pure state or as one of the phases in the case of phase separation. No solution with coexistence of SF and CDW in the same homogeneous state has, instead, been found.

III. MEAN FIELD THEORY ANALYSIS

A. Strong-coupling mean-field theory

In this section, we describe analytical mean-field calculations for both weak and strong couplings which help in understanding the DMFT phase diagram established numerically. We first present a *strong-coupling* analysis, which holds for $|U| \gg t_\uparrow, t_\downarrow$. In order to analyze this limit, we find it useful to resort to a particle-hole transformation (Table I) that maps our negative- U model onto the positive- U Hubbard model and work in the repulsive- U framework. We emphasize that we are not switching to truly repulsive interactions, but we simply exploit a mathematical property to gain information on the physical system of our interest. Under this mapping, our model is transformed, at large $|U| \gg t_\uparrow, t_\downarrow$, into an XXZ quantum spin-1/2 model:^{2,5}

$$H = J \sum_{\langle i,j \rangle} \vec{S}_i \cdot \vec{S}_j + \gamma J \sum_{\langle i,j \rangle} S_i^z S_j^z - h \sum_i (2S_i^z - m), \quad (5)$$

TABLE I. Particle-hole transformation mapping the $U < 0$ model with $\langle n_\uparrow \rangle = \langle n_\downarrow \rangle$ onto a half-filled $U > 0$ model with a magnetic field.

$- U < 0$	$ U > 0$
$c_{i\uparrow}^\dagger, c_{i\downarrow}^\dagger$	$d_{i\uparrow}^\dagger, (-1)^i d_{i\downarrow}$
$n_{c\uparrow}, n_{c\downarrow}$	$n_{d\uparrow}, 1 - n_{d\downarrow}$
$\delta \equiv n_c - 1 = \langle n_{c\uparrow} + n_{c\downarrow} \rangle - 1$	$m_d = \langle n_{d\uparrow} - n_{d\downarrow} \rangle$
Chemical potential μ_c	Field $h_d = \mu_c - U /2$
h_c	$\mu_d = h_c + U /2$
SF: $\langle c_{i\uparrow}^\dagger c_{i\downarrow}^\dagger \rangle$	SDW _{xy} : $\langle (-1)^i \langle d_{i\uparrow}^\dagger d_{i\downarrow} \rangle$
CDW: $\langle (-1)^i \langle \hat{n}_{ci} \rangle$	SDW _z : $\langle (-1)^i \langle S_{di}^z \rangle$

in which $\vec{S} \equiv \frac{1}{2} d_\alpha^\dagger \vec{\sigma}_{\alpha\beta} d_\beta$, $J = 4t_\uparrow t_\downarrow / |U|$, and $\gamma = (t_\uparrow - t_\downarrow)^2 / 2t_\uparrow t_\downarrow = 2z^2 / (1 - z^2)$. Hence, the mass imbalance turns into a spin exchange anisotropy. The uniform magnetic field h corresponds to the original chemical potential $\mu - |U|/2$ and the magnetization to the doping δ (Table. I). The mean-field approach¹¹ amounts for treating the spin variables as classical and minimizes the energy over the angles θ_A, θ_B describing the orientation of the spins in the two sublattices. The energy per site reads (with ζ the lattice connectivity and $c_{A,B} \equiv \cos \theta_{A,B}$ and $s_{A,B} \equiv \sin \theta_{A,B}$)

$$\frac{E}{N} = \frac{\zeta}{8} J s_A s_B + \frac{\zeta}{8} J (1 + \gamma) c_A c_B - \frac{h}{2} [c_A + c_B - 2m]. \quad (6)$$

The phase diagram is characterized by the competition between the xy spin-density wave (SDW_{xy}) with order parameter $\Delta_{xy} = \langle (-1)^i S_i^y \rangle$ (corresponding to SF ordering for $U < 0$), and Néel order (SDW_z) $\Delta_z = \langle (-1)^i S_i^z \rangle$ (corresponding to CDW). The solution changes according to the magnetization m of the system (i.e., the doping of our physical model). The m vs h curve has a discontinuity of amplitude $m_c = \sqrt{\gamma / (\gamma + 2)} = z$. For $m=0$ (half-filling $\delta=0$), a SDW_z (CDW) state is obtained. For $m \in [m_c, 1]$, the homogeneous SDW SDW_{xy} (SF) state is stable, while for $0 < m < m_c$ phase separation takes place between the two types of ordering. Thus, when working at fixed magnetization (corresponding to fixed doping δ), one finds a SF for $z < z_c = m = \delta$ and phase separation for $z > z_c = \delta$. This strong-coupling value (indicated by arrows in Fig. 1) agrees very well with our DMFT results.

B. Weak-coupling mean-field theory

We now turn to the opposite weak-coupling limit. We decouple the interaction term in the SF and the CDW channels and determine the regions of stability of each phase. We first consider the BCS decoupling of the interaction, introducing the order parameter $\Delta_{BCS} = (|U|/N) \sum_{\mathbf{k}} \langle c_{\mathbf{k}\uparrow}^\dagger c_{\mathbf{k}\downarrow}^\dagger \rangle$ to make the Hamiltonian quadratic. In Nambu formalism, it reads

$$H_{BCS} = \sum_{\mathbf{k}} \psi_{\mathbf{k}}^\dagger \begin{bmatrix} \xi_{\mathbf{k}\uparrow} & -\Delta_{BCS} \\ -\Delta_{BCS} & -\xi_{\mathbf{k}\downarrow} \end{bmatrix} \psi_{\mathbf{k}} + E_G. \quad (7)$$

Here, $\tilde{\mu}_\sigma \equiv \mu - U n_{-\sigma}$, $\xi_{\mathbf{k}\sigma} = \varepsilon_{\mathbf{k}\sigma} - \tilde{\mu}_\sigma$, and $E_G = \sum_{\mathbf{k}} \xi_{\mathbf{k}\downarrow} + N|U|n_\uparrow n_\downarrow + N\Delta_{BCS}^2 / |U|$. The diagonalization of Eq. (7)

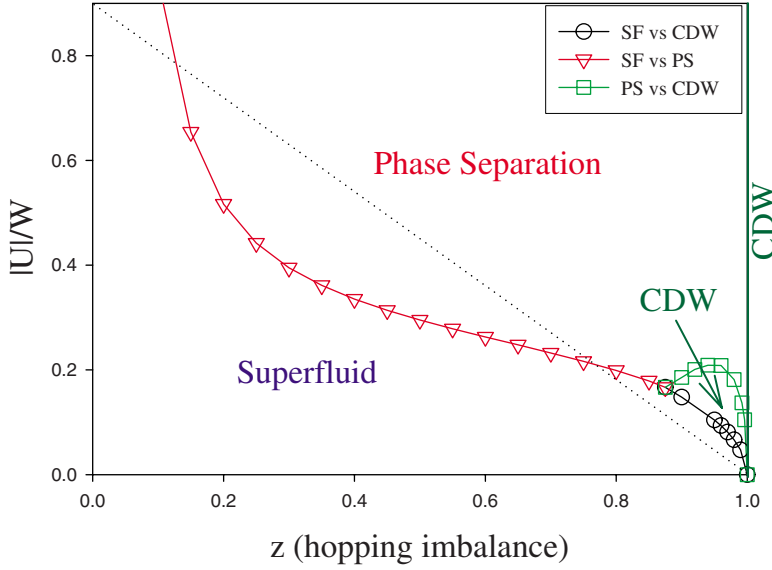


FIG. 2. (Color online) Phase diagram for $\delta = 0.05$ from weak-coupling mean field (whose validity is questionable above the dotted line) (see text). For simplicity, a square density of states was used here.

yields the Bogoliubov modes with eigenvalues $E_{\mathbf{k}}^{\pm} = \pm(\xi_{\mathbf{k}\uparrow} - \xi_{\mathbf{k}\downarrow})/2 + \sqrt{(\xi_{\mathbf{k}\uparrow} + \xi_{\mathbf{k}\downarrow})^2/4 + \Delta_{\text{BCS}}^2}$. Defining new variables $\xi_{\mathbf{k}} = (\xi_{\mathbf{k}\uparrow} + \xi_{\mathbf{k}\downarrow})/2$ and $\tilde{\mu} = (\tilde{\mu}_{\uparrow} + \tilde{\mu}_{\downarrow})/2$, the usual form of the BCS gap equation is recovered. We can readily compute the energy of BCS phase, obtaining $E_{\text{BCS}} - E_n = -\Delta_{\text{BCS}}^2/2W$, which tells us that the normal state is always unstable toward SF ordering.

Analogously, we can decouple the interaction in the CDW channel defined by the order parameter $\Delta_{\sigma} = (|U|/N)\sum_{\mathbf{k}}\langle c_{\mathbf{k}+\mathbf{Q}\sigma}^{\dagger}c_{\mathbf{k}\sigma} \rangle$ with $\mathbf{Q} = (\pi, \pi, \pi)$. Introducing the spinor $\psi_{\mathbf{k}\sigma}^{\dagger} = (c_{\mathbf{k}\sigma}^{\dagger}, c_{\mathbf{k}+\mathbf{Q}\sigma}^{\dagger})$, the mean-field Hamiltonian reads

$$H_{\text{CDW}} = \sum_{\mathbf{k} \in \text{RBZ}, \sigma} \psi_{\mathbf{k}\sigma}^{\dagger} \begin{bmatrix} \varepsilon_{\mathbf{k}\sigma} - \tilde{\mu}_{\sigma} & -\Delta_{\sigma} \\ -\Delta_{\sigma} & -\varepsilon_{\mathbf{k}\sigma} - \tilde{\mu}_{\sigma} \end{bmatrix} \psi_{\mathbf{k}\sigma} + E_0, \quad (8)$$

with $E_0 = N\Delta_{\uparrow}\Delta_{\downarrow}/|U| + N|U|n_{\uparrow}n_{\downarrow}$. It is readily diagonalized, with eigenvalues, $E_{\mathbf{k}\sigma}^{\pm} = \pm\sqrt{\varepsilon_{\mathbf{k}\sigma}^2 + \Delta_{\sigma}^2} - \tilde{\mu}_{\sigma}$. This yields the following two self-consistent conditions:

$$\frac{1}{N} \sum_{\mathbf{k} \in \text{RBZ}} [f(E_{\mathbf{k}\sigma}^{+}) + f(E_{\mathbf{k}\sigma}^{-})] = n_{\sigma},$$

$$\frac{\Delta_{\sigma}}{N} \sum_{\mathbf{k} \in \text{RBZ}} \frac{f(E_{\mathbf{k}\sigma}^{-}) - f(E_{\mathbf{k}\sigma}^{+})}{\sqrt{\varepsilon_{\mathbf{k}\sigma}^2 + \Delta_{\sigma}^2}} = \frac{\Delta_{-\sigma}}{|U|}. \quad (9)$$

At a fixed value of the chemical potential, these CDW equations have the following solutions: (i) for all $|U|$ and z , a normal solution with $\Delta_{\text{CDW}} = 0$, which is unstable toward SF; (ii) for large enough $|U|$, a half-filled (commensurate) CDW; and (iii) for large values of z close to 1, a homogeneous CDW solution is also found with a density different from unity ($\delta \neq 0$).

We first compare the ground-state energies of the two mean-field solutions: the homogeneous SF and the SF/half-filled CDW phase-separated solution obtained from a Maxwell construction. The resulting phase boundary (Fig. 1) is seen to be qualitatively reasonable and even quantitatively

accurate (in comparison to the numerical DMFT result) for some intermediate range of z . Indeed, the weak-coupling mean field is justified only when $|U| \lesssim t_{\uparrow}, t_{\downarrow}$, i.e., $|U|/W \lesssim (1-z)$.¹² An indicative line below which weak-coupling static mean field is reliable is shown in panel (b) of Fig. 3

In Fig. 2, we perform a more detailed comparison of the ground-state energies of three mean-field solutions: the homogeneous SF, the phase-separated SF/CDW, and the homogeneous CDW with $\delta \neq 0$ (when it exists). This comparison yields a small region of parameters, for large z , in which a homogeneous CDW with a density different from one atom per site is stable. The phase transition between SF and CDW could be studied by a more sophisticated mean-field approach allowing simultaneously for both CDW and BCS orders. Within this approach, a different scenario from a first-order transition can be realized. Namely, CDW and BCS orders can coexist in the same solution for some range of parameters, giving rise to a supersolid phase, which here becomes favored by the presence of the underlying optical lattice. In light of the absence of a supersolid state in DMFT, we did not consider this possibility in the weak-coupling mean-field theory.

IV. LOCAL DENSITY APPROXIMATION FOR THE HARMONIC TRAP POTENTIAL

We finally discuss the effect of the trap potential. For simplicity, we perform an explicit calculation only in the strong-coupling limit, using again the particle-hole transformation (Table 1) and considering the effective spin model [Eq. (5)]. A harmonic trap potential yields a position-dependent chemical potential which corresponds under the particle-hole transformation to a spatially varying magnetic field $h(r) = h - h_0 r^2/R_0^2$. Here, R_0 is the radius of the circular trap, $h_0 = m\omega_0^2 R_0^2/2$, and $h = \mu - |U|/2$ is related to the chemical potential at the center of the trap, which must be adjusted so that the local density $n(r)$ integrates to the total number of atoms. We start from a local density approximation (LDA) and also compare with a Monte Carlo solution of the strong-

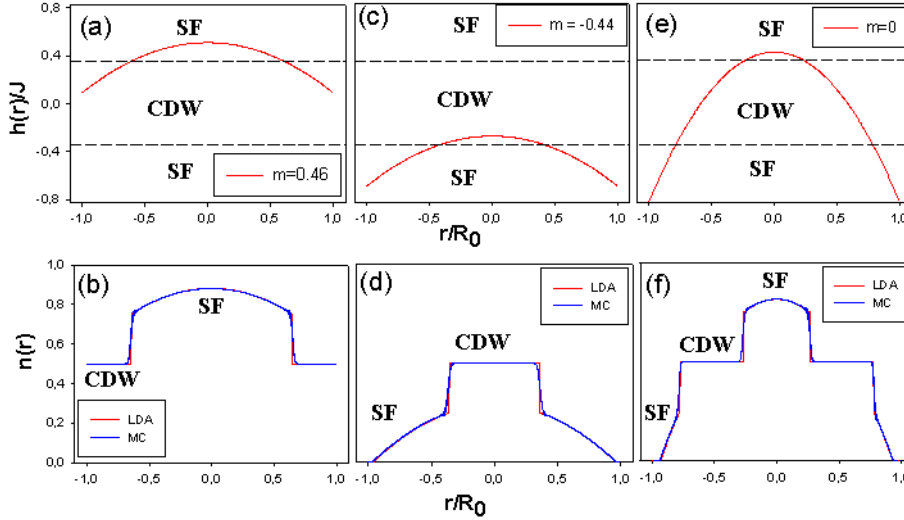


FIG. 3. (Color online) Density profiles and domains with different orderings inside the trap (bottom panels), as discussed in text. The top panels show how the trap potential intersects the characteristic values of the chemical potential in each case.

coupling model in the presence of $h(r)$. As described above, the strong-coupling analysis of the uniform system yields a critical magnetic field (chemical potential) at which $m(h)$ is discontinuous. For $|h| < h_c = J\zeta\sqrt{\gamma(\gamma+2)} = \frac{8z\zeta}{1-z^2} \frac{t_1 t_2}{|U|}$, we have a SDW_z (CDW) phase; otherwise we have a SDW_{xy} (SF) phase. Within the LDA approximation, this implies that in a region where $|h(r)|$ is smaller (larger) than h_c , we locally observe SDW_z/CDW ordering ($\text{SDW}_{xy}/\text{SF}$). According to the values of the parameters h and h_0 , and noting that $h - h_0 < h(r) < h$, one finds several different regimes:

(i) $h - h_0 > h_c$ or $h < -h_c$. The trap potential is always larger than h_c , or smaller than $-h_c$, so that the system is in a SDW_{xy} (SF) phase everywhere inside the trap, and the density profile varies smoothly.

(ii) $h > h_c$ and $|h - h_0| < h_c$. In this case, $h(r) > h_c$ inside a circle of radius $R_1 = R_0\sqrt{(h - h_c)/h_0}$ centered at $r = 0$. Hence, one has phase separation into two distinct regions: SDW_{xy} (SF) ordering within this circle and SDW_z (CDW) in the outer ring (Fig. 3, left panel).

(iii) $h - h_0 < -h_c$ and $|h| < h_c$. We find again phase separation with the opposite spatial arrangement. The SDW_{xy} (SF) part is stable out of a circle of radius $R_2 = R_0\sqrt{(h + h_c)/h_0}$, inside which there is a SDW_z (CDW) phase (Fig. 3, middle panel).

(iv) $h > h_c$ and $h - h_0 < -h_c$. Then, the magnetic field profile crosses both h_c and $-h_c$, so that there are three spatial regions: $R < R_1$ where we find SDW_{xy} (SF), then the ring $R_1 < r < R_2$ where SDW_z (CDW) establishes, and finally an outer ring $r > R_2$ with SDW_{xy} (SF) ordering (Fig. 3, right panel).

In the three last cases [(ii)–(iv)], in which phase separation occurs, the LDA approximation predicts a jump of the magnetization at the phase boundaries R_1 and R_2 , corresponding to a jump of the density in the original $U < 0$ model (see also Refs. 13). In order to test this prediction and assess the validity of LDA, we performed a classical Monte Carlo simulation of model [Eq. (5)] in the presence of a spatially

dependent field $h(r)$. For simplicity, this test was performed in a one-dimensional geometry. We find a remarkable agreement between the LDA density profiles and the Monte Carlo solution, which confirms that very sharp variations of the local density indeed takes place at the boundary between domains in cases [(ii)–(iv)].

V. CONCLUSION

In this paper, we have studied the phase diagram of mixtures of fermionic atoms with different masses in a cubic optical lattice in the case in which the interaction is attractive. For small values of the unbalance, the system remains in a homogeneous superfluid phase, exactly as in the case of equal masses. When the anisotropy exceeds a given critical value, which depends on the density of fermions, the system is a pure superfluid only in weak coupling, and increasing the coupling determines a phase separation between a superfluid state and a commensurate charge density wave, in which an alternated pattern of atoms is observed. Once the harmonic trap potential is taken into account, the phase separation is actually realized in different regions of the trap (for example, the superfluid can be present in the central region, while the density wave is confined to the outer part of the trap), with rapid variations of the local density at the phase boundaries. We note finally that, in the case of the ${}^6\text{Li}/{}^{40}\text{K}$ mixture, a simple estimate shows that the mass imbalance z can be varied over a large range by changing the lattice depth V_0/E_R ($z \ll 1$ at small V_0/E_R and $z \approx 0.9$ for $V_0/E_R \approx 15$), so that the effects discussed in this work can indeed be actually observable in these systems.

ACKNOWLEDGMENTS

We are grateful to I. Carusotto, F. Chevy, P. S. Cornaglia, T. Giamarchi, D. Rohe, C. Salomon, and F. Schreck for useful discussions. Support was provided by the ANR under “GASCOR,” and by CNRS, Ecole Polytechnique and MIUR-PRIN under Project No. 200522492.

- ¹D. Jaksch and P. Zoller, *Ann. Phys.* **315**, 52 (2005); W. Zwerger, *J. Opt. B: Quantum Semiclassical Opt.* **5**, 9 (2003); I. Bloch, *Nat. Phys.* **1**, 24 (2005); A. Georges, arXiv:cond-mat/0702122 (unpublished).
- ²M. A. Cazalilla, A. F. Ho, and T. Giamarchi, *Phys. Rev. Lett.* **95**, 226402 (2005).
- ³W. V. Liu and F. Wilczek, *Phys. Rev. Lett.* **90**, 047002 (2003); M. Iskin and C. A. R. Sa de Melo, *ibid.* **97**, 100404 (2006).
- ⁴F. Werner, O. Parcollet, A. Georges, and S. R. Hassan, *Phys. Rev. Lett.* **95**, 056401 (2005).
- ⁵L.-M. Duan, *Phys. Rev. Lett.* **95**, 243202 (2005).
- ⁶Innsbruck group (private communication).
- ⁷C. A. Stan, M. W. Zwierlein, C. H. Schunck, S. M. F. Raupach, and W. Ketterle, *Phys. Rev. Lett.* **93**, 143001 (2004).
- ⁸A. Georges, G. Kotliar, W. Krauth, and M. J. Rozenberg, *Rev. Mod. Phys.* **68**, 13 (1996).
- ⁹M. Keller, W. Metzner, and U. Schollwöck, *Phys. Rev. Lett.* **86**, 4612 (2001); M. Capone, C. Castellani, and M. Grilli, *ibid.* **88**, 126403 (2002); B. Kyung, A. Georges, and A.-M. S. Tremblay, *Phys. Rev. B* **74**, 024501 (2006).
- ¹⁰A. Toschi, P. Barone, M. Capone, and C. Castellani, *New J. Phys.* **7**, 7 (2005); A. Toschi, M. Capone, and C. Castellani, *Phys. Rev. B* **72**, 235118 (2005).
- ¹¹R. T. Scalettar, G. G. Batrouni, A. P. Kampf, and G. T. Zimanyi, *Phys. Rev. B* **51**, 8467 (1995).
- ¹²J. K. Freericks and V. Zlatic, *Rev. Mod. Phys.* **75**, 1333 (2003).
- ¹³G.-D. Lin, W. Yi, and L.-M. Duan, *Phys. Rev. A* **74**, 031604(R) (2006).
- ¹⁴The DMFT equations were solved using exact diagonalization (Ref. 8), with eight energy levels in the effective bath.